

Spin-polarized tunneling effects observed on the oxygen-terminated Fe_3O_4 (111) surface

N. Berdunov,^{a)} S. Murphy, G. Mariotto, and I. V. Shvets
SFI Nanoscience Laboratory, Trinity College, Dublin 2, Ireland

Y. M. Mykovskiy
MISIS, Leninsky Prospect 4, Moscow 119991, Russia

(Presented on 7 January 2004)

Under oxidizing preparation conditions the magnetite (111) surface reconstructs to a highly ordered superlattice. This surface reconstruction represents an oxygen termination of the magnetite bulk. We employ spin-polarized (SP) scanning tunneling magnetization (STM) to study the spin-dependent tunneling between a magnetite (111) sample and an antiferromagnetic tip through a vacuum barrier. Atomic scale STM images show significant magnetic contrast corresponding to variations in the local surface states induced by oxygen vacancies. The local variations of the tunneling magnetoresistance around these vacancies correspond to 150%. By employing SP-STM measurements and first principles calculations we could conclude that an oxygen top layer considerably changes the SP properties of the magnetite surface. © 2004 American Institute of Physics. [DOI: 10.1063/1.1688643]

INTRODUCTION

Magnetite, Fe_3O_4 , predicted to be a half-metallic ferromagnet, attracts a lot of interest from the spin electronics community. It is expected that a magnetic tunnel junction (MTJ) with a Fe_3O_4 electrode could exhibit a high tunneling magnetoresistance (TMR) effect. In practice, at room temperature such MTJs do not demonstrate a sizable magnetoresistance and at low temperature the MR values reported are still much lower than expected.¹ However, the photoelectron spectroscopy measurements on the magnetite surface do show much greater values of the spin polarization (SP).² It was suggested that this reduction of SP is due to the disorder at the electrode/barrier drastically changing the spin-polarized properties of the interface.³ In complex structures, like magnetite, the surface can possess a number of nonidentical terminations, which have a variety of spin-electronic properties. For example, it was shown that an oxygen layer deposited on a magnetic electrode could change MTJ properties drastically, even reversing the sign of spin polarization.⁴ Therefore, an understanding of the relationship between spin-electronic properties and the structure of the surfaces/interfaces at the nanometer and atomic scale is of much interest.

In the present work we apply SP scanning tunneling microscopy (SP-STM) measurements to analyze the electronic structure of the oxygen-terminated magnetite (111) surface. We aim to understand the impact of point defects on the

surface electronic structure and on the spin dependent tunneling between a magnetite sample and an antiferromagnetic MnNi tip through a vacuum barrier. The potential of SP-STM as a useful tool to study the surface magnetic properties has been demonstrated in recent experimental and theoretical works.⁵ Spin-dependent tunneling can be achieved by selecting the tunneling conditions for the majority and minority spin states. SP-STM techniques can be broadly divided into two groups. The first one utilizes a soft ferromagnetic tip with the magnetization switched by an applied local magnetic field.⁶ However, there are no reports of atomic resolution achieved with this approach so far. The second one uses an antiferromagnetic tip to scan the surface where the magnetic field applied is strong enough to alter the sample magnetization. In earlier theoretical work⁷ it has been shown that spin contrast can be achieved in the case of tunneling between an antiferromagnet and ferromagnet electrodes. The first experiments have been reported in Ref. 8. More recently, atomically resolved SP-STM data employing Cr and MnNi tips have been reported.^{9,10}

To analyze the SP properties of the oxygen-terminated magnetite (111) surface we have performed density functional theory (DFT) calculations for the ideal oxygen-terminated magnetite (111) vacuum slab (vacuum/magnetite/vacuum interface). The CASTEP algorithm within the local spin-density approximation was used to optimize the surface geometry, first, and then calculate the local density of states.

RESULTS AND DISCUSSION

The experiments have been performed in ultrahigh vacuum (UHV) at room temperature, using STM, low-

^{a)} Author to whom correspondence should be addressed; electronic mail: nikolay.berdunov@tcd.ie

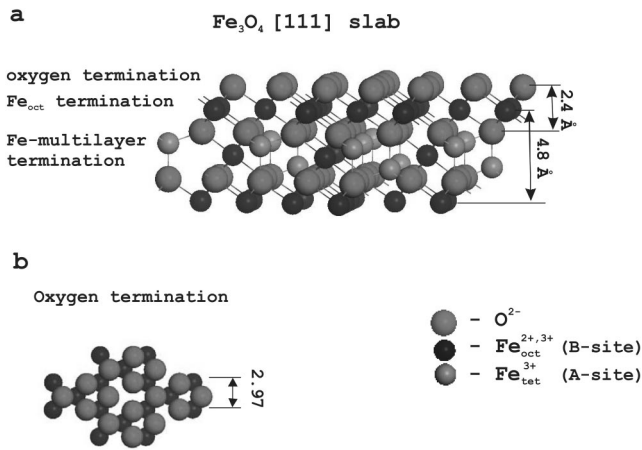


FIG. 1. Magnetite [111] vacuum slab (a) and oxygen termination on the top of Fe octahedral layer (b).

energy electron diffraction (LEED), and Auger spectroscopy. In our SP–STM measurements, MnNi tips made of antiferromagnetic alloy were employed. The tip preparation is discussed in detail in Ref. 11. A magnetite (111) synthetic single crystal has been used in these experiments. The crystal structure of magnetite allows for six ideal bulk terminations in the (111) plane (Fig. 1). Two of them represent terminations consisting of close-packed oxygen layers and the other four are surface planes containing Fe^{2+,3+} cations. One of the two oxygen terminations appears as an oxygen monolayer on top of an octahedral Fe layer, while the other covers a multilayer of tetrahedral and octahedral Fe atoms. The atomic periodicities of both oxygen terminations are identical [Fig. 1(b)].

As each termination corresponds to a different subsurface stoichiometry, by choosing either a reduction or an oxidation sample preparation procedure, we were able to achieve two stable terminations. One is referred to in Ref. 12 as the Fe-tetrahedral termination, another represents an oxygen termination with a long-range order on the surface.

Oxygen-Induced Surface Reconstruction

The magnetite sample was annealed in UHV followed by a short anneal in an oxygen atmosphere of 10^{-6} mbar at 950 K for 15 min, which was in turn followed by cooling in

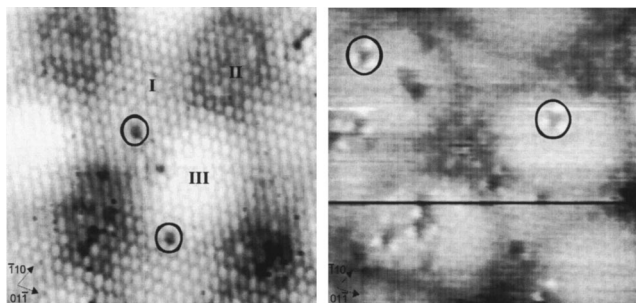


FIG. 2. STM images ($9 \times 8 \text{ nm}^2$) of the superstructure without (a) and with magnetic field (b). The circles mark the missing oxygen defects in the topmost surface layer. In a case of the applied magnetic field, three bright spots appeared around defect correspond to the Fe sites with 6 Å interatomic distance ($V_{\text{bias}} = -1.0 \text{ V}$, $I_t = 0.1 \text{ nA}$, MnNi tip in both cases).

an oxygen atmosphere. This sample preparation procedure leads to the formation of a well-defined hexagonal superlattice with a periodicity of 42 Å. This superstructure is highly regular and covers almost the entire sample surface. The high-resolution STM image in Fig. 2(a) shows the atomic arrangement within the superstructure. One can see that the superstructure consists of three distinct areas, marked I, II, and III. Detailed analysis shows that area I has a periodicity of 3.1 Å, while areas II and III have a periodicity of 2.8 Å along the [011] direction, which is consistent with the LEED pattern. As we have shown in an earlier publication,¹³ the superstructure constitutes an oxygen-terminated magnetite bulk, which reconstructs due to an electron-lattice instability, polaron, or charge density wave like. Thus, the STM image in Fig. 2(a) represents a lattice of oxygen sites on top of an iron layer. A number of defects seen in Fig. 2(a) represent the missing oxygen atoms. We have further shown¹⁴ that at a critical density of oxygen vacancies of some 30%, the superstructure disappears. This means that the topmost oxygen layer is responsible for the electronic transformation in the subsurface layer, and for the Fe state changes leading to the superstructure formation.

In our SP–STM experiments a magnetic field of 60 mT was applied parallel to the surface during the STM scan. We have verified by vibrating sample magnetometry that this magnetic field is strong enough to fully saturate the magnetization of the sample. The contrast achieved in STM images when the magnetic field is switched off/on is demonstrated in Figs. 2(a) and 2(b), respectively. It can be seen that the appearance of the superstructure and corrugation between different areas is almost unaffected by the magnetic field. However, major changes occur in the proximity of the oxygen vacancies. Three bright spots appear in the vicinity of the defect, as can be seen in Fig. 2(b). A 6 Å separation between the spots and their relative positions correspond to those of Fe ions in the layer underneath the topmost oxygen lattice.

We can quantify the observed spin polarized effect in terms of the tunneling conductance variation¹⁵ around the surface defects

$$\sigma = (G_{60 \text{ mT}} - G_0) / G_0, \quad (1)$$

where $G_{60 \text{ mT}}$, G_0 are the tunneling conductances with and without the applied magnetic field. To estimate the tunneling conductances, we can use a simplified approach where the tunnel current is a function of the bias voltage U , the distance d , and the energy of the barrier φ between the two electrodes

$$I_t \sim (U/d_i) \exp(-A\varphi_i^{-1/2}d_i),$$

where index $i=1,2$ corresponds to the case when the tip is positioned above an oxygen vacancy and above an oxygen atom, respectively. In our experiment, the tunnel current is $I_t = 0.1 \text{ nA}$, the bias voltage $U = 1 \text{ V}$. The tip displacement over the point of the corrugation maxima in the STM image is equal to 0.3 Å. Assuming that the tip–surface distance is 5 Å, we can calculate the change in the barrier energy and the corresponding tunnelling conductance of the 5 Å tunnelling gap. Their substitution into formula (1) gives us a σ value of 1.5. This value indicates a significant TMR effect of up to

150% in the presence of the defects (oxygen vacancies) on the surface. Although in the absence of a magnetic field it is not necessarily true that we fulfill the conditions for the minimum conductance, and therefore the calculated TMR value should be taken as the lower limit.

It is known that in transition metals the $3d$ electrons make a large contribution to the tunneling current. In the case of the oxygen-terminated surface, one may not expect a tunneling contribution from the oxygen p states. However, on the surface the hybridization between oxygen p states and transition metal d states alters the oxygen p orbitals from insulating to conductive.¹⁶ The results of our DFT calculations support this viewpoint: the oxygen states on the magnetite surface contribute to the tunneling at negative bias. The layer-projected partial density of states shows significant $p-d$ state hybridization between the topmost oxygen anions and the Fe ions in the layer underneath. The p states of the oxygen anions are shifted towards the Fermi level eliminating the band gap. This effect almost disappears in the second oxygen layer, where the oxygen p states are similar to those in the bulk. These predictions are in good agreement with our experimental data. We readily resolve the 3 \AA periodicity of the oxygen sites at bias voltages ranging from -1 to -0.5 V, while this lattice disappears if we tunnel in/from the surface states about and above Fermi level (bias from -0.3 to $+1$ V). The absence of the Fe lattice in STM images taken at positive bias (tunnelling to the unoccupied Fe states) can be explained by scattering of the tunneling electrons in a closed-packed oxygen layer. While in the case of the oxygen vacancies present on the surface, the Fe states become prominent.

CONCLUSIONS

Investigating the tunnelling between an oxygen-terminated Fe_3O_4 (111) surface and an antiferromagnetic tip

across a vacuum barrier, we observed significant changes in TMR values, which are localized in the vicinity of oxygen vacancies on the surface.

We conclude that a surface oxygen layer plays a decisive role in the spin-polarized properties of the magnetite interface, which consists of the reduction of spin polarization in the case of the closed oxygen layer on the surface.

ACKNOWLEDGMENT

This work was supported by Science Foundation of Ireland (SFI) under Contract No. 00/PI.1/C042.

¹G. Hu and Y. Suzuki, *Phys. Rev. Lett.* **89**, 276601 (2002).

²Yu. S. Dedkov, U. Rüdiger, and G. Güntherodt, *Phys. Rev. B* **65**, 064417 (2002).

³J. S. Moodera, J. Nowak, and J. M. van de Veerdonk, *Phys. Rev. Lett.* **80**, 2941 (1998).

⁴I. I. Oleynik and E. Y. Tsymbal, *J. Appl. Phys.* **93**, 6429 (2003).

⁵H. F. Ding, W. Wulfhekel, J. Henk, P. Bruno, and J. Kirschner, *Phys. Rev. Lett.* **90**, 116603 (2003).

⁶M. Bode, *Rep. Prog. Phys.* **66**, 523 (2003).

⁷A. Minakov and I. V. Shvets, *Surf. Sci.* **236**, L377 (1990).

⁸I. V. Shvets, R. Wiesendanger, D. Burgler, G. Tarrach, H. J. Guntherodt, and J. M. D. Coey, *J. Appl. Phys.* **71**, 5489 (1992).

⁹A. Kubetzka, M. Bode, O. Pietzsch, and R. Wiesendanger, *Phys. Rev. Lett.* **88**, 057201 (2002).

¹⁰G. Mariotto, S. Murphy, and I. V. Shvets, *Phys. Rev. B* **66**, 245426 (2002).

¹¹S. F. Ceballos, G. Mariotto, S. Murphy, and I. V. Shvets, *Surf. Sci.* **523**, 131 (2003).

¹²Sh. K. Shaikhutdinov, M. Ritter, X.-G. Wang, H. Over, and W. Weiss, *Phys. Rev. B* **60**, 11062 (1999).

¹³I. V. Shvets, N. Berdunov, G. Mariotto, and S. Murphy, *Europhys. Lett.* **63**, 867 (2003).

¹⁴N. Berdunov, S. Murphy, G. Mariotto, and I. V. Shvets, *Phys. Rev. B* (submitted, 2003).

¹⁵M. Jullier, *Phys. Lett.* **54A**, 225 (1975).

¹⁶E. Y. Tsymbal, O. N. Mryasov, and P. R. LeClair, *J. Phys.: Condens. Matter* **15**, R109 (2003).